Development of Low Cost Industrially Scalable PCM Capsules for Thermal Energy Storage in CSP Plants

Start Date – December 2011

D. Yogi Goswami, Ph.D, PE
Distinguished University Professor
Director, Clean Energy Research Center
University of South Florida, Tampa, FL 33620

USF UNIVERSITY OF SOUTH FLORIDA

CERC Clean Energy Research Center

arpa·e

Development Goal and Approach

Develop very low cost industrially scalable capsules of PCMs for utility scale TES for CSP plants operating at 300^0C to 1000^0C

APPROACH

- Use low cost, high temperature PCMs with uniquely tailored heat transfer characteristics for overcoming the problem of low thermal conductivity of PCMs for fast charging and discharging
- Optically active PCMs and shell linings for enhanced heat transfer
- Use electroless deposition techniques for encapsulating the porous PCM pellets to form capsules of required size and shape

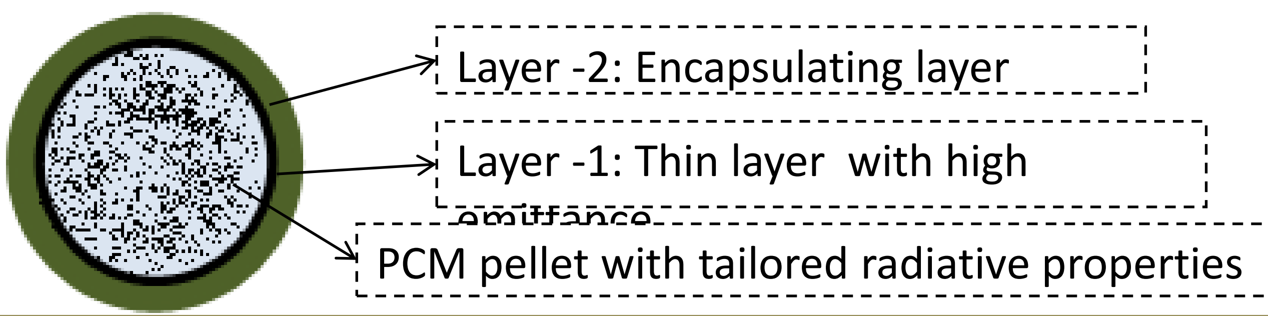

Properties of some phase change materials of interest

PCM	Melting point (^{0}C)	Latent Heat (kJ/kg)
$NaNO_3$	308	172*
KCl(22)-50MgCl2-30NaCl	396	291
NaCl(56.2)-43.8MgCl2	442	325
CaCl2(52.8)-47.2NaCl	500	239
KCl(45)-55KF	605	407
NaCl(50)-50KCl	657	338*
K2CO3(51)-49Na2CO3	710	163
NaCl	801	510*

* Experimental measured values.
All salt concentrations are in mole percent.

Encapsulation of PCM pellets (300 - 400^{0}C)

- **Precoating – A layer is coated around the salt pellet**
- **The pre-coat is metallized using electroless and electroplating chemistry**

Final PCM Capsule for 300 – 400^0 C range

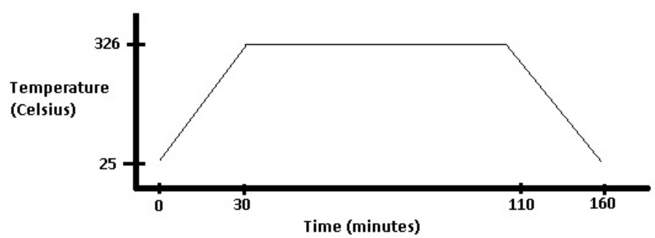

Capsule after 1500 Thermal Cycles ~ 5 years equivalent

Characterization of PCMs

No of cycles passed	Melting point Tm (° C)	Heat of Fusion (j/g)
0	307.2	170.2
59	306.82	170.6
154	308.15	170.3
700	306.56	170.7
1000	307.47	170.6

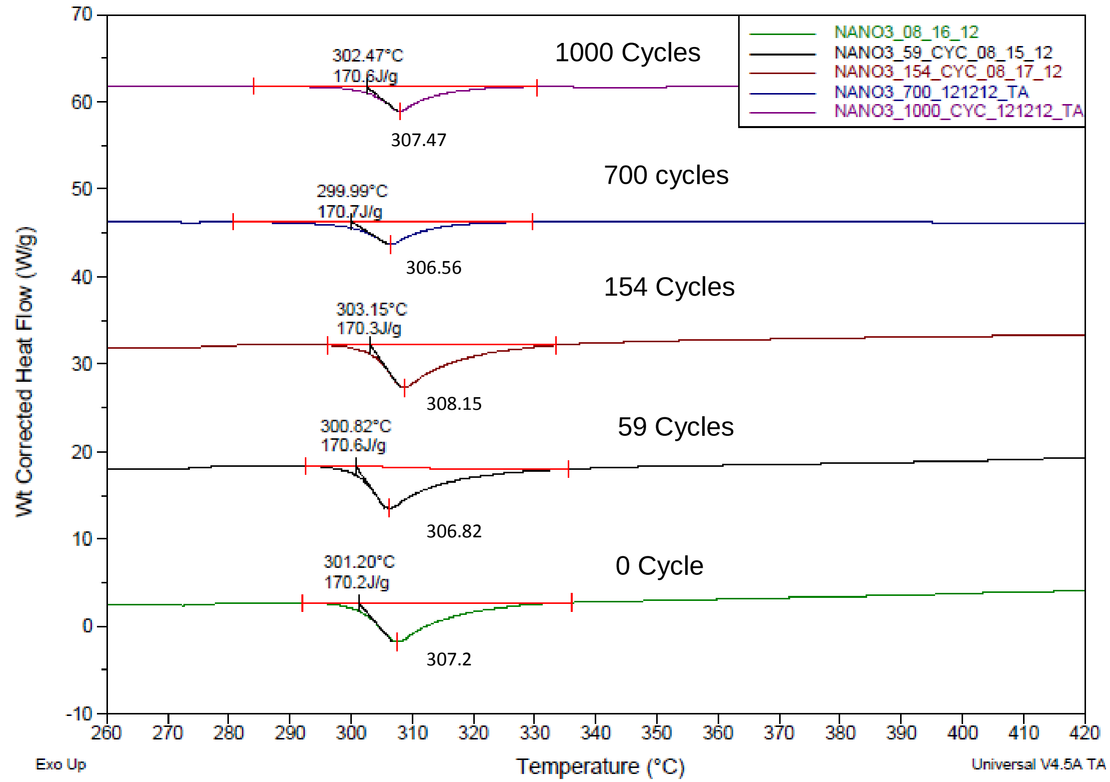

Development of Coating Procedures for 600-1000^{0}C Capsules

Two methods are being developed the High Temperature PCMs

- **The first method involves the Use of preformed ceramic shells.**

Pre-formed ceramic shells

Final encapsulated PCM

Development of Coating Procedures for 600-1000^{0}C Capsules

❑ **The second method involves direct ceramic coating on the salt pellet**

Thermal testing was done on the capsules at 805^{o}C. The pellet was cut open to check for leakage of salt into the pores of the ceramic layer.

NaCl capsule coated with the ceramic

Intact salt capsule after thermal testing

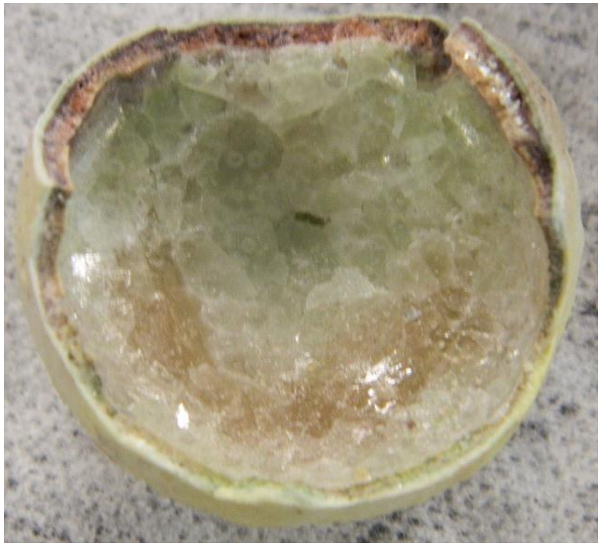

Cut portion of the capsule

Development of Coating Procedures

An electroless and electrochemical deposition of metal over the ceramic layer is being developed. This is to reduce the overall thickness of the ceramic layer and give strength to the pellet.

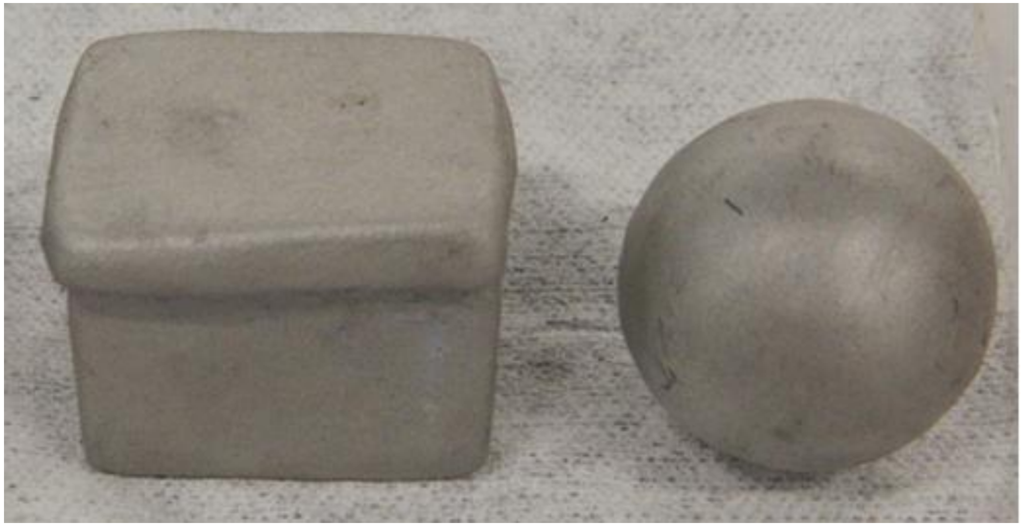

Pre-formed ceramic shell with metal layer

Demonstration of Improved Radiative Heat Transfer

- Nano-scale additive attenuates radiation in the infrared region (left fig.)
- DSC demonstrates improved heat transfer in KCl-NaCl eutectic.
  - Small concentration (0.3 wt %) yields pronounced *increase in heat flow rate* (right fig. vertical axis).
  - Shift in peaks suggests *accelerated melt time*.

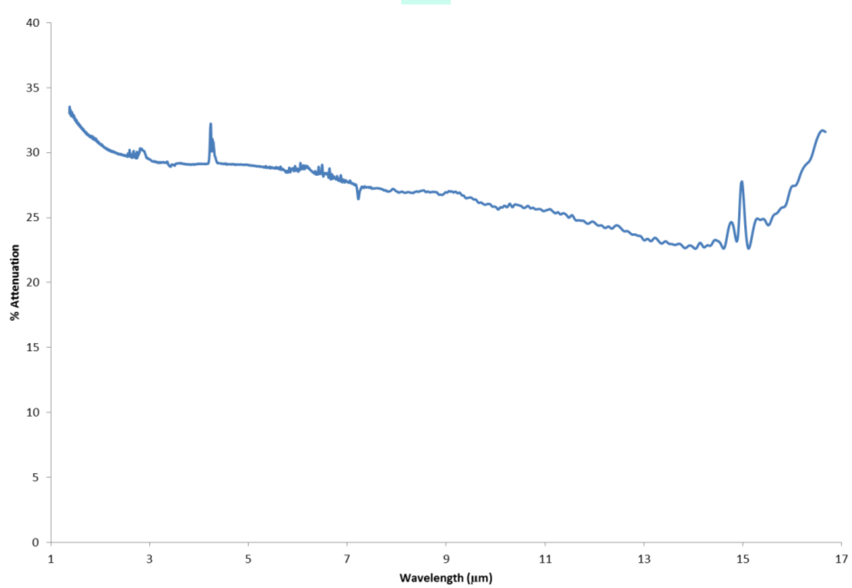

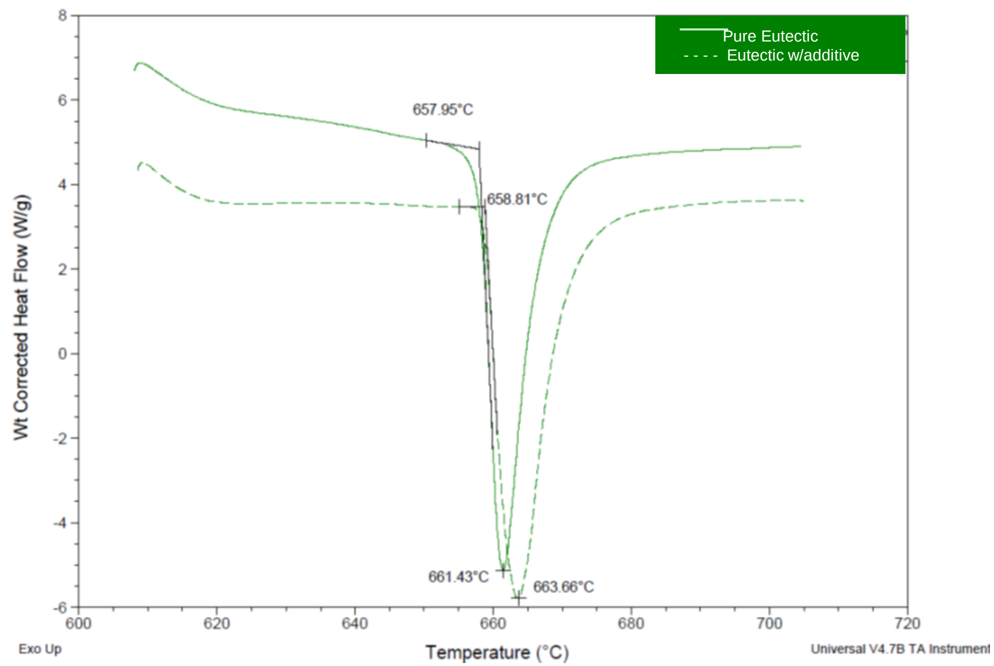

Demonstration of Improved Radiative Heat Transfer

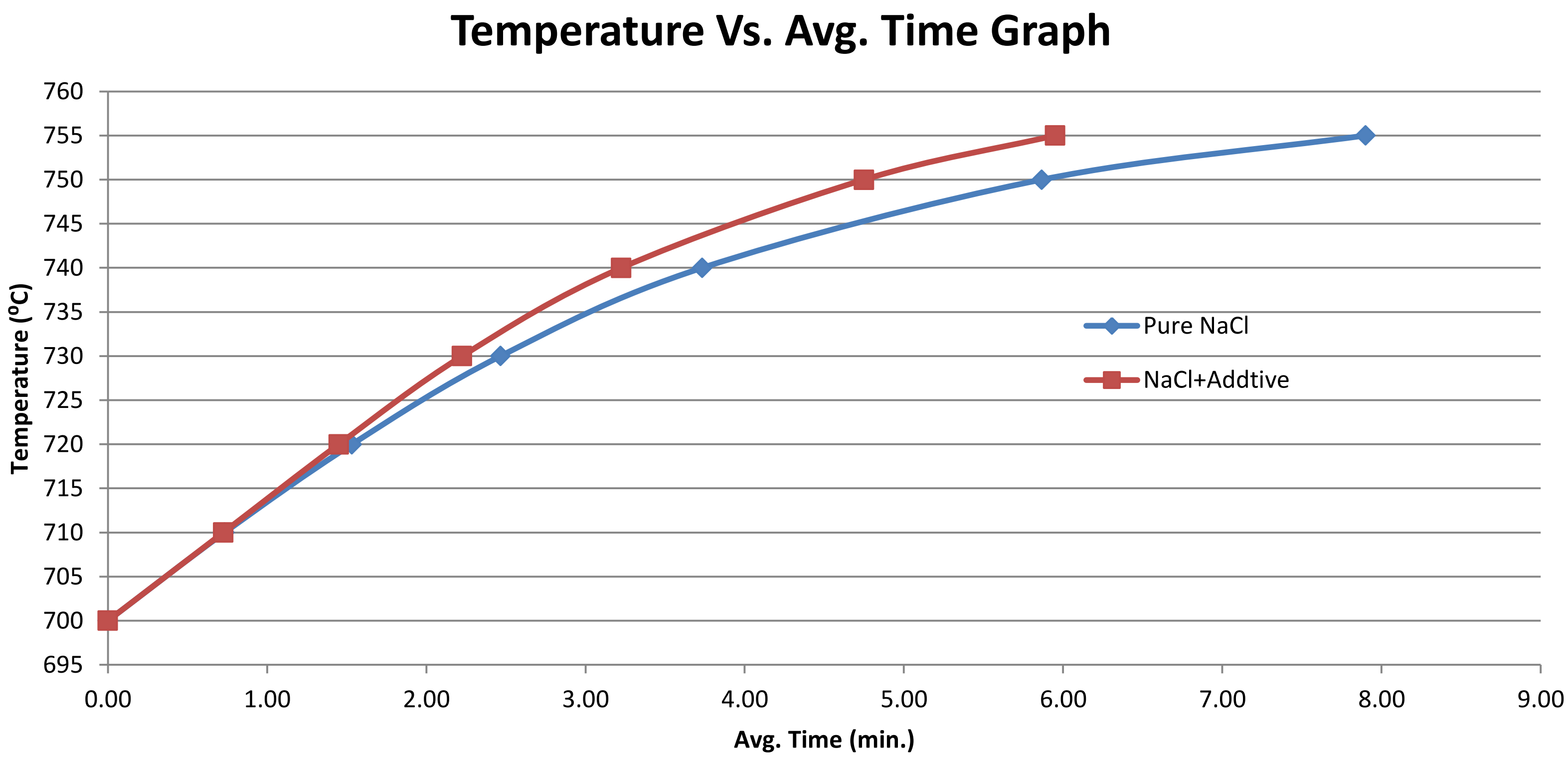

Characterization of the PCMs

Latent Heat of the chosen PCMs (NaCl and 50%NaCl-50%KCl eutectic) were measured using TA Instruments DSC-TGA (see eutectic endotherm below)

- ΔH_{fus} (NaCl) = 509.91 J/g ΔH_{fus} (eutectic) = 337.6 J/g

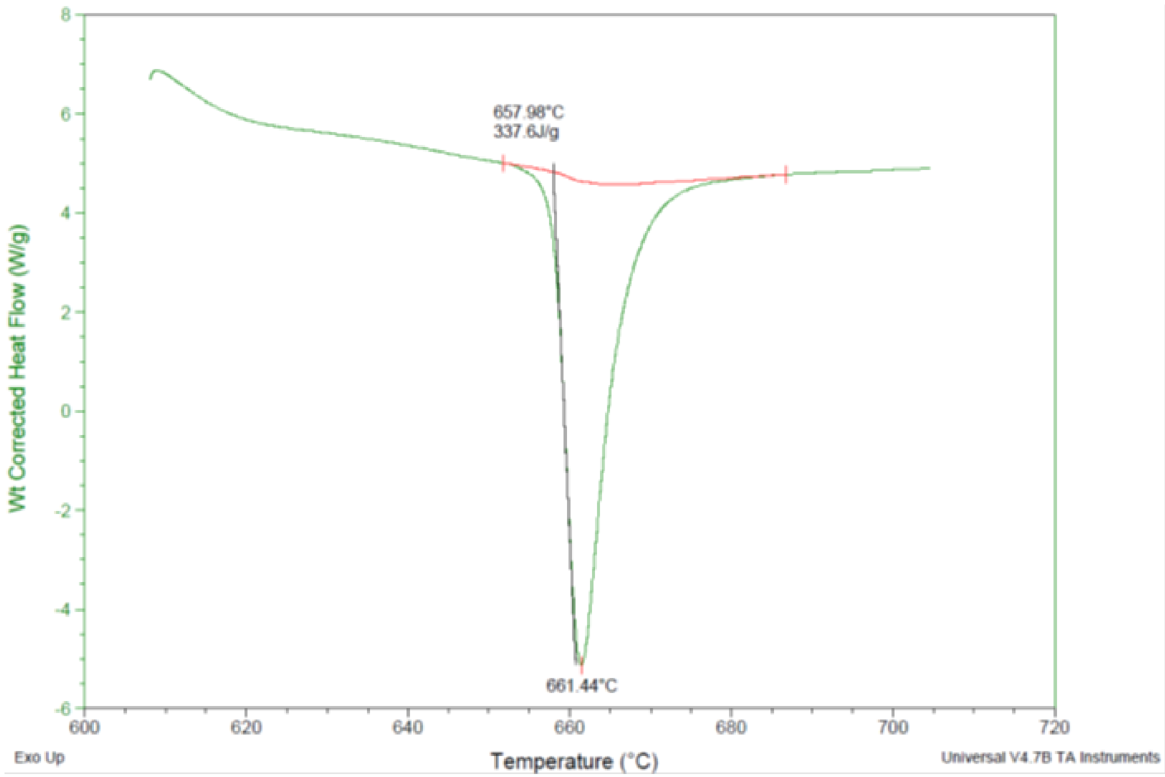

Cyclic Testing and Evaluation of the PCM Pellets

- High temperature capsules are undergoing heating and cooling cycles.
- Optimization of ceramic composition and thickness is in progress.

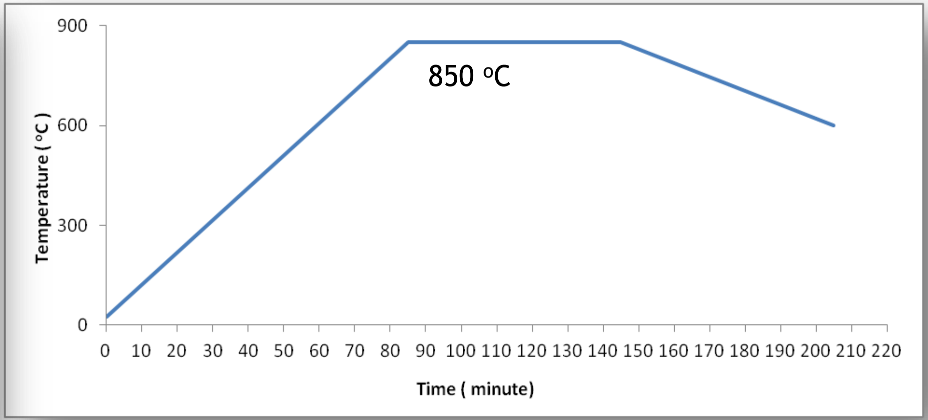

The pellet was cut open to check the diffusion of the salt into the ceramic layer

Manufacturing Process Layout

1 Screw Feeder for PCM powder

2 Homogenizer/Mixer/ Vibrating Shaker/ Hopper

Mesh at the bottom for the flow of uniform size particle distribution

Conveyor belt for carrying uniform size powder

Important quality control steps required during each subsequent processing steps:
1) Monitoring or a continuous flow through feeder
2) Particle size distribution; Quality of mixing
3) Size; Strength; Weight loss
4) Thermal cycling of PCM

3 Production of pellets in Rotary press

4 Pre-coating Thermal treatment (Surface preparation before coating)

5 Coating on PCM in impaction blending dry particle coating machine

6 Post-coating Thermal treatment (IR Heater)

7 Electroless coating involving a series of sub-processing steps

8 Electroplating involving a series of sub-processing steps

Preliminary cost analysis

PCM system	Material cost ($/kWh$_{th}$)	Processing cost (30%)	Tank cost ($/kWh$_{th}$)	System cost ($/kWh$_{th}$)
PCM-1	13.30	3.99	3.14	**20.43**
PCM-2	9.04	2.71	3.14	**14.89**
PCM-3	7.70	2.31	3.14	**13.15**
PCM-4	8.47	2.54	3.14	**14.16**

Numerical Results

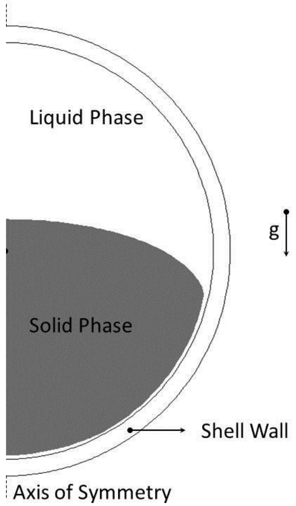

Fig. 1 System schematic.

Property	NaCl
$Density\ (kg/m^3)$	
$solid\ phase$	2160
$mushy\ zone$	$325858.7 - 302T$
$Liquid\ phase$	$2139.3 - 0.543T$
$\rho_l (kg/m^3)$	1556
$Dynamic\ viscosity\ (kg/m\ s)$	$1.01x10^{-3}$
$Latent\ heat\ of\ fusion\ (J/kg)$	479289
$Melting\ temperature\ (°C)$	800.7
$Specific\ heat\ (J/kgK)$	1200
$Thermal\ conductivity\ (W/mK)$	0.7

Table1. Thermo-physical properties.

- A spherical shell, is entirely filled with the solid NaCl at T_i =797.7 ^{o}C. For time t>0, a constant temperature boundary condition T_w (10, 15 and 20 ^{o}C above the NaCl melting temperature, 800.7 ^{o}C) is applied on the outer surface of the shell. Fig. 1 shows the schematic of the system

- The PCM is treated as a semitransparent medium where thermal radiation can be emitted and absorbed. Physical properties are presented in Table 1.

Numerical Results

- A number of non-dimensional quantities and parameters can be defined to characterize the heat transfer and the phase change process at high temperatures. Those are:

$$Gr = \frac{g\beta(T_w - T_m)R_i^3}{\nu^2} \qquad Pl = \frac{k(\kappa_a + \kappa_s)}{4\sigma T_0^3}$$

$$Pr = \frac{\nu}{\alpha} \qquad Ste = \frac{C_p(T_w - T_m)}{L} \qquad \alpha = \frac{k}{\rho c_p}$$

$$T_0 = \frac{T_w + T_m}{2}$$

$Gr = Grashof\ number$ | $\beta = thermal\ expansion\ coeff.$

$Pl = Planck\ number$ | $k = Thermal\ conductivity$

$Pr = Prandtl\ number$ | $\kappa_a = absorption\ coefficient$

$Ste = Stefan\ number$ | $\kappa_s = scattering\ coefficient$

$c_p = specific\ heat$ | $\nu = Kinematic\ viscosity$

$R_i = shell\ inner\ radius$ | $\theta = dimensionless\ temp.$

$g = gravity$ | $\rho = Density$

$L = latent\ heat$ | $\sigma = Stefan - Boltzmann\ ctn.$

$\propto = thermal\ diffusivity$ | $T_0 = reference\ temp.$

- Different study cases have been analyzed for a 15mm inner radius capsule in order to asses the effects of the wall temperature and absorption coefficient (k_a) on the thermal performance of the system. All of them are summarized in Table 2.

Table2. Study cases.

Case	T_w - T_m (ºC)	Gr_R	Ste	$k_a(m^{-1})$	Pr
1	10	$2.75x10^5$	0.025		
2	15	$4.12x10^5$	0.037	100	1.74
3	20	$5.48x10^5$	0.050		
4	20	$5.48x10^5$	0.050	20	1.74
5	10	$2.75x10^5$	0.025	0	

Numerical Results

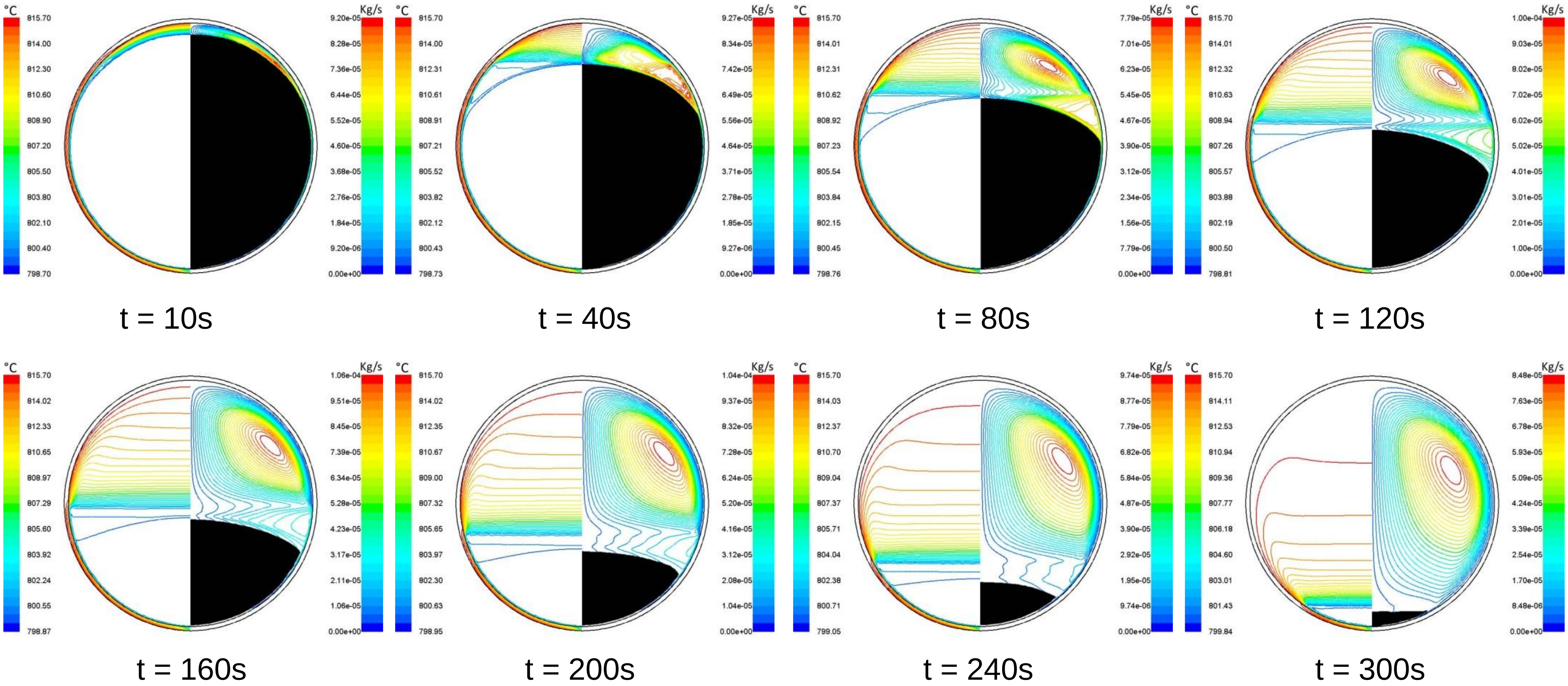

Fig. 2 Predicted evolution of the solid fraction, isotherms and streamline contours.

The predicted isotherms (left), streamlines contours (right) and PCM solid phase distribution (right) during the melting of a 30mm internal diameter capsule (case2), as a function of time are presented in composite diagrams shown in this Figure. Shell thickness is 0.5mm and shell material is a Nickel alloy.

Numerical Results

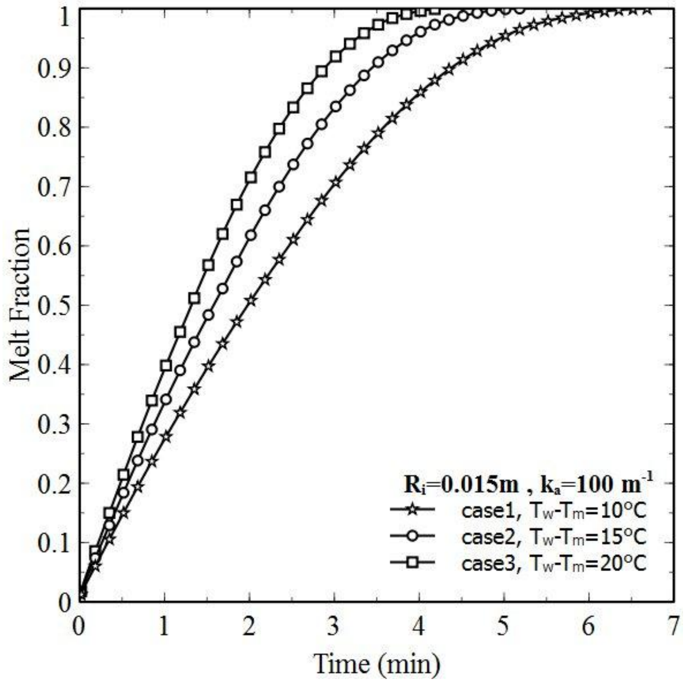

Fig. 3 Effect of the outer temperature.

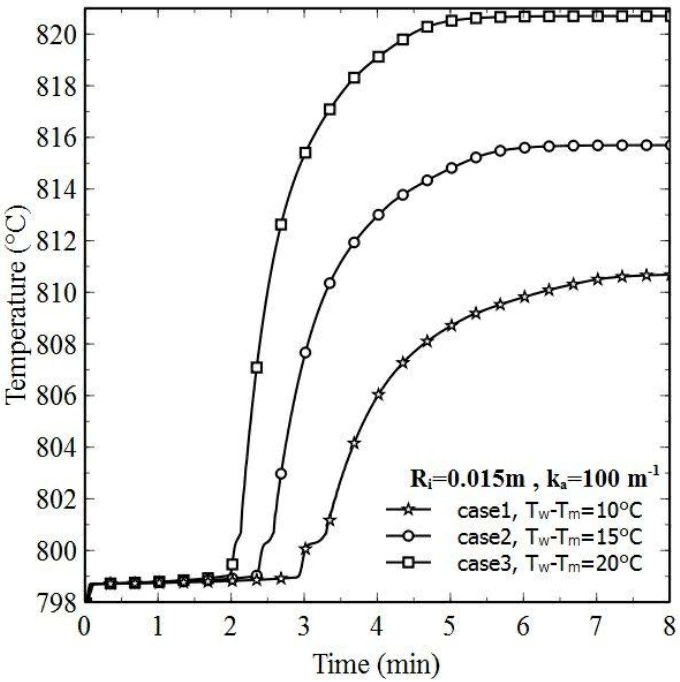

Fig. 4 Center point temperature history.

The effect of the outer wall temperature on the predicted melt fraction rate is depicted in Fig. 3.
Faster melting is achieved when the wall temperature increases. The total melting time is reduced by 36% when the outer wall temperature increases from 10 to 20^{o}C above the NaCl melting temperature.

The predicted temperature history at the center point of the container for different outer wall temperatures is presented in Fig. 4.
As expected faster response is obtained when the outer wall temperature increases.

Numerical Results

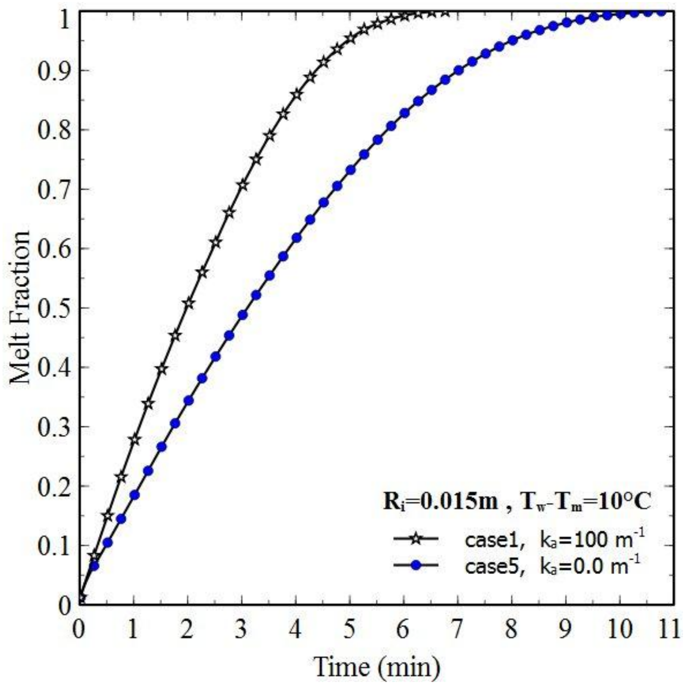

Fig. 5 Melt fraction rate for cases 1 and 5.

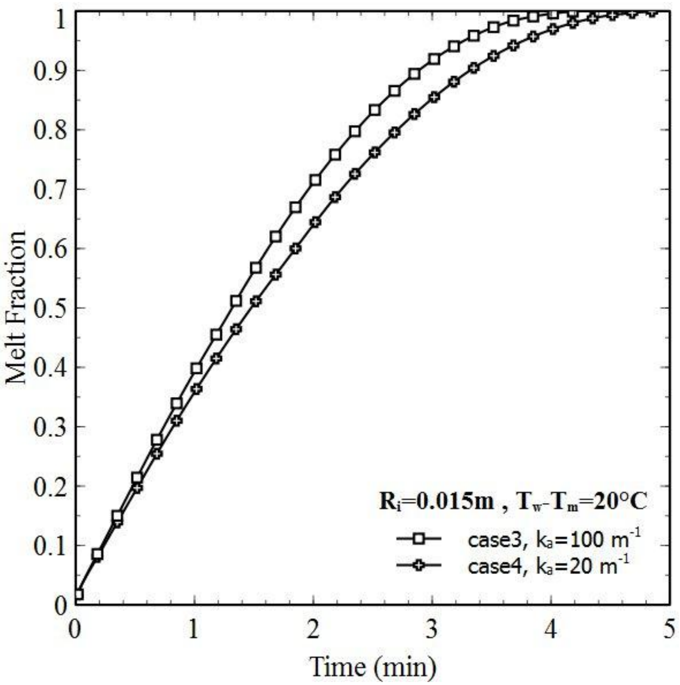

Fig. 6 Effect of the absorption coefficient.

The predicted melt fraction rate for study cases 1 and 5 are presented in fig. 5.
Faster melting is observed in the case where NaCl is treated as an absorbing and emitting medium. The total melting time is reduced by 35% when the absorption coefficient increases from 0 to 100m^{-1}

The effect of the absorption coefficient (k_a) on the predicted melt fraction rate is shown in Fig. 6.
Faster melting is achieved when the absorption coefficient is higher.

Numerical Results

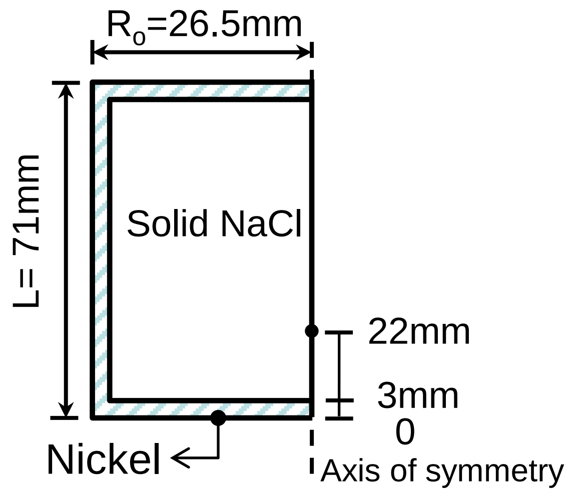

Fig. 7. Schematic of the system.

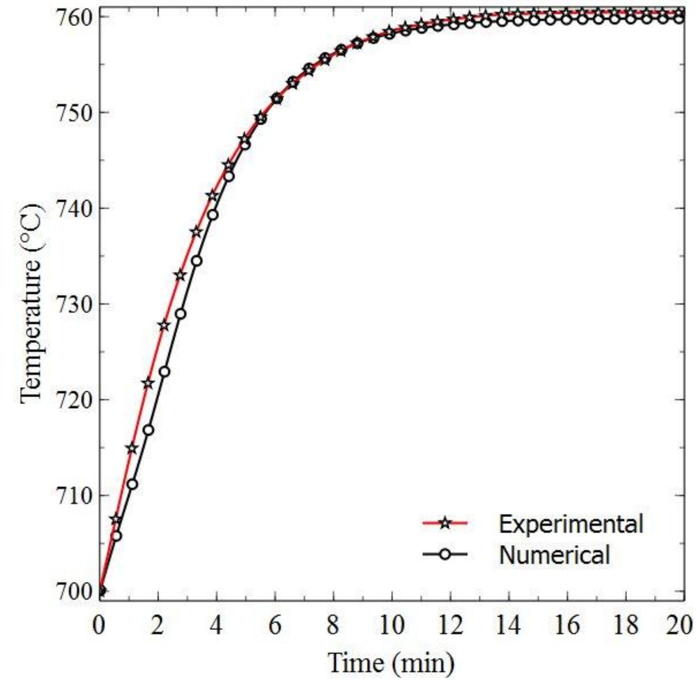

Fig. 8. Time history at shown location.

- Vertical cylindrical container (Fig. 7) is initially filled with solid NaCl at 700° C. For time t>0 a constant temperature boundary condition (T_w=760° C) is imposed at the outer surface of the wall.
- The transient diffusion-controlled heat transfer is analyzed. The numerically predicted and the experimentally measured temperature history at 19mm above the bottom surface of the container is presented in Fig.8.
- The numerically predicted time history shows a good agreement with experimental results.

USF UNIVERSITY OF SOUTH FLORIDA CERC Clean Energy Research Center arpa·e

Numerical Results

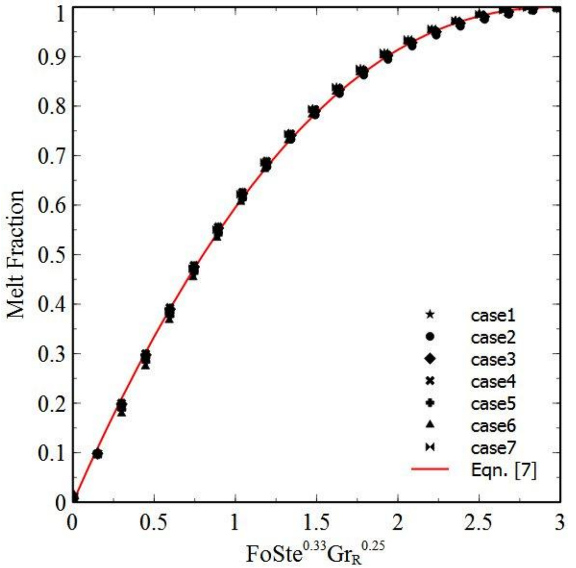

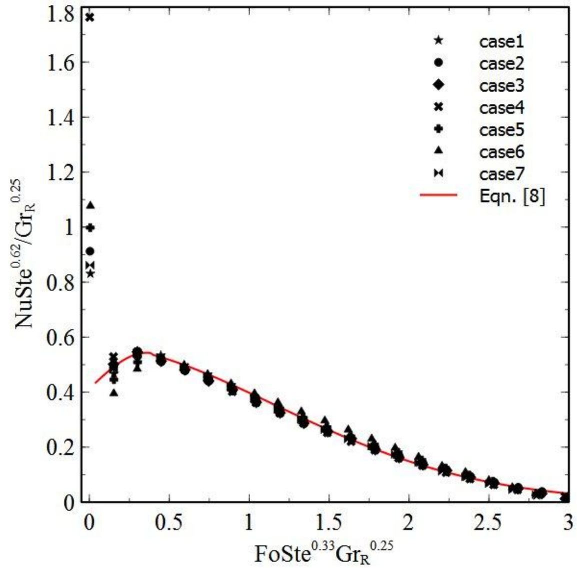

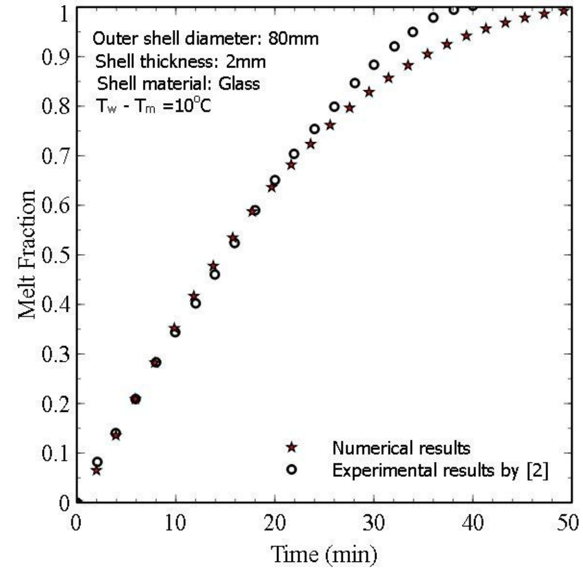

Melt Fraction rate correlation.

Dimensionless Nusselt number

Validation case

$$MF = 1 - \left[1 - \frac{FoSte^{0.33}Gr_R^{0.25}}{3}\right]^{2.23} \qquad [7]$$

$$\frac{NuSte^{0.62}}{Gr_R^{0.25}} = \begin{cases} 0.345exp(-5.75\xi^{3.25}) + \sin(0.068 + 0.55\xi), & 0.04 \le \xi < 0.4 \\ 0.57exp(-0.36\xi^{1.9}), & 0.4 \le \xi \le 3.0 \end{cases} \qquad [8]$$

Correlations valid in the range encompassing the cases simulated:
$0.047 < Ste < 0.104$, $1.28 \times 10^4 < Gr_R < 2.0 \times 10^5$, $Pr = 9.1$.

[2] Assis E, Katsman L, Ziskind G, Letan R. Numerical and experimental study of melting in a spherical shell. Int J Heat Mass Transfer 2007; 50: pp. 1790–1804.

Conclusions

- Successfully developed PCM capsules with provision for expansion/contraction during melting/freezing

- Characterized the PCMs of interest

- Tested capsules for thermal cycling
  - Completed 1500 cycles (continuing) for 300 – 400^0C
  - Capsules for 600 – 1000^0C being optimized for cyclic performance

- Developed a numerical model for melting/solidification

- Developed a manufacturing plan for capsules

- Cost estimate of a TES system based on the developed PCM capsules – $\$13.15/\text{kWh}_{th}$ (<< than goal of $\$20$)

FUTURE WORK

- Optimization of ceramics coatings for encapsulation
- Continuation of Thermal cyclic testing of capsules
- Development of a numerical model for System Design
- Continuation of Characterization of PCMs and Capsules
- Testing in a lab scale TES system

Thank You